Antitumor Agents

DOI: 10.1002/anie.201400763

Organotin(IV)-Loaded Mesoporous Silica as a Biocompatible Strategy in Cancer Treatment**

*Mirna Z. Bulatović, Danijela Maksimović-Ivanić, Christian Bensing, Santiago Gómez-Ruiz, Dirk Steinborn, Harry Schmidt, Marija Mojić, Aleksandra Korać, Igor Golić, Damian Pérez-Quintanilla, Miljana Momčilović, Sanja Mijatović, and Goran N. Kaluđerović**

Abstract: *The strong therapeutic potential of an organotin(IV) compound loaded in nanostructured silica (SBA-15pSn) is demonstrated: B16 melanoma tumor growth in syngeneic C57BL/6 mice is almost completely abolished. In contrast to apoptosis as the basic mechanism of the anticancer action of numerous chemotherapeutics, the important advantage of this SBA-15pSn mesoporous material is the induction of cell differentiation, an effect unknown for metal-based drugs and nanomaterials alone. This non-aggressive mode of drug action is highly efficient against cancer cells but is in the concentration range used nontoxic for normal tissue. JNK (Jun-amino-terminal kinase)-independent apoptosis accompanied by the development of the melanocyte-like nonproliferative phenotype of survived cells indicates the extraordinary potential of SBA-15pSn to suppress tumor growth without undesirable compensatory proliferation of malignant cells in response to neighboring cell death.*

Cisplatin is one of the most effective and commonly used agents to treat various types of human cancer.[1] Despite the great therapeutic success of cisplatin, some cancer cells relatively rapidly acquires resistance or are intrinsically resistant to cisplatin, leading to relapse and therapeutic failure.[2] The use of high-dose cisplatin regimens in the treatment of most aggressive malignancies lacking effective treatment, such as cisplatin-resistant melanoma,[3] has been shown to be effective in advanced cases but is always associated with unacceptable side effects.[4] The goal in developing new metal-based anticancer drugs is to overcome the main limitations of cisplatin, such as its narrow range of activity, the development of resistance, and its severe toxicity.[5]

Apoptosis is the basic mechanism of the anticancer action of numerous chemotherapeutics. Alternatively, the most important action of chemotherapeutics is the induction of cell differentiation as an opposite process to malignant transformation. There are numerous naturally occurring compounds as well as synthetic drugs with antitumor action based on this process,[6] but metal-based compounds causing this type of transformation are still undiscovered. This approach has not yet been exploited and the induction of apoptosis is still the favored mechanism of oncotherapy even though this means of cell death causes a strong signal for the proliferation of surrounding anaplastic cells. This phenomenon known as compensatory proliferation was found to be connected with enhanced JNK activation.[7]

In recent years, the application of nanotechnology in medicine has pointed toward drug delivery, imaging, and other therapeutic and diagnostic applications.[8] Nanoparticles have been developed to treat diseases at the cellular level and to apply drug therapies that might be targeted to malignant tissues.[9] Many of these nanomaterials require difficult synthetic methods and the incorporation of photoresponsive molecules or target receptors.[10]

Nanostructured silica-based materials are already highly promising candidates in several fields of medicine, but in cancer therapy there have been relatively few investigations.[11] These materials are nontoxic to cells,[12] have large external surfaces and porous cores, and may be functionalized with small molecules and used as drug carriers.[13] However, the in vivo antitumor effect of nanostructured silica loaded with metal compounds is still unknown.

Some of us have previously reported that loading of bioinactive mesoporous nanomaterials with cytotoxic titanocene

[*] C. Bensing, Prof. D. Steinborn, Dr. H. Schmidt, Prof. G. N. Kaluđerović
Institut für Chemie
Martin-Luther-Universität Halle-Wittenberg
Kurt-Mothes-Strasse 2, 06120 Halle (Germany)
E-mail: goran.kaluderovic@chemie.uni-halle.de
Prof. G. N. Kaluđerović
Department of Bioorganic Chemistry
Leibniz Institute of Plant Biochemistry
Weinberg 3, 06120 Halle (Saale) (Germany)
M. Z. Bulatović, Dr. D. Maksimović-Ivanić, Dr. M. Mojić, Dr. M. Momčilović, Dr. S. Mijatović
Institute for Biological Research "Sinisa Stankovic"
University of Belgrade
Bulevar despota Stefana 142, 11060 Belgrade (Serbia)
Prof. S. Gómez-Ruiz, Dr. D. Pérez-Quintanilla
Departamento de Química Inorgánica y Analítica
E.S.C.E.T., Universidad Rey Juan Carlos
28933 Móstoles, Madrid (Spain)
Prof. A. Korać, I. Golić
Center for Electron Microscopy, Faculty of Biology
University of Belgrade
Studentski trg 16, 11000 Belgrade (Serbia)

[**] We thank the Ministry of Education, Science and Technological Development of Serbia (grant no. 173013) and the Ministerio de Economía y Competitividad, Spain (grant no. CTQ2012-30762) for financial support.

Supporting information for this article (including materials, preparation of $Ph_3Sn(CH_2)_6OH$, SBA-15p, and SBA-15pSn, cell lines, animals, and used) is available on the WWW under http://dx.doi.org/10.1002/anie.201400763.

derivatives enhances their activity in tumor cells.[14] In the current study, we selected SBA-15 mesoporous silica as a carrier, because of its higher cytotoxicity upon loading with titanium compounds (compared to that of MCM-41 loaded with titanium compounds).[14] Because triphenyltin(IV) compounds express high activities (compared both to titanocene derivatives and cisplatin),[14,15] we present here the strong therapeutic potential of the nanostructured material SBA-15 loaded with an organotin(IV) compound.

SBA-15 was synthesized by a sol–gel method and a subsequent calcination step (see the Supporting Information).[14] SBA-15p particles were prepared by covalent grafting of SBA-15 with 3-chloropropyltriethoxysilane (CPTS). The extent of the functionalization with attached $\equiv Si(CH_2)_3Cl$ units was calculated from the chlorine content (XRF) as 0.76 mmol Cl per g SiO_2. The content of carbon is higher than expected from the Cl content, pointing to an incomplete substitution of ethoxy groups in the reaction of CPTS with SBA-15. This was further confirmed by ^{13}C CP MAS and ^{29}Si MAS NMR spectroscopic investigations. Besides functionalization of the external surface of the nanomaterial, the inner surface was also functionalized, as confirmed by ^{13}C CP MAS and ^{29}Si MAS NMR spectra, by the decrease of pore size and BET surface, and the increase of the wall thickness in direct comparison to SBA-15 (Table S1). Based on the calcination temperature of SBA-15 (500 °C) it could be estimated that the functionalization gave a mixture of singly and doubly grafted molecules.[16] SEM and TEM images of SBA-15p did not show any significant difference to those of SBA-15, implying that the morphology of the material was not affected by functionalization with CPTS (Figure 1).

Treatment of SBA-15p with 6-triphenylstannylhexan-1-ol yielded SBA-15pSn particles, which are loaded with the organotin(IV) compound. XRD analysis showed a loading of 0.324 mmol Sn per g SiO_2. As expected, the pore size observed in SBA-15pSn (4.80 nm) was smaller than that in SBA-15p (4.88 nm) and in SBA-15 (4.97 nm). A small amount of $Ph_3Sn(CH_2)_6OH$ is located on the external surface of the material, as evident by the decrease of the surface area. Organotin(IV) loading was confirmed by solid-state NMR spectroscopy. Besides the resonance pattern (^{13}C CP MAS) of 3-chloropropyl groups, aromatic and methylene resonances were found corresponding to $Ph_3Sn(CH_2)_6OH$. In the ^{119}Sn MAS NMR spectrum, a singlet resonance (−106 ppm) arises from $Ph_3Sn(CH_2)_6OH$ (for further details see the Supporting Information). SEM and TEM images of SBA-15pSn (Figure 1) showed a uniform morphology of nanostructured rods (particle size ca. 720×460 nm, calculated from SEM data) and a uniform pore size (hexagonal form).

For investigations of the in vitro activity, B16 tumor cells were cultivated in the presence of $Ph_3Sn(CH_2)_6OH$, SBA-15pSn, and SBA-15p at a wide range of dosages, and cell viability was estimated by MTT and CV tests after 48 and 72 h. Treatment of cells with $Ph_3Sn(CH_2)_6OH$ resulted in dose-dependent inhibition of cell viability (Figure S7). Interestingly, the IC_{50} value calculated from MTT experiments ($IC_{50} = 20$ μM) was half of that obtained from the CV test ($IC_{50} = 40$ μM). This discrepancy lays in the fact that disturbance of mitochondrial respiration as a consequence of toxic stimulus results in the reduction of cellular viability (Figure S7). On the other hand, treatment of cells with SBA-15pSn (3.85 % Sn) resulted in a remarkable decrease of cell viability ($M_{50} = 2\ \mu g\,mL^{-1}$ from MTT and $2.6\ \mu g\,mL^{-1}$ from CV assay). The advantage of the novel SBA-15pSn over the most active titanium-loaded mesoporous material (SBA-15 loaded with the $[Ti\{Me_2Si(\eta^5\text{-}C_5Me_4)(\eta^5\text{-}C_5H_4)\}Cl_2]$, $M_{50} = 309 \pm 42\ \mu g\,mL^{-1}$) from the previous study,[14] is that its in vitro activity is more than 150 times higher.

The amount of $Ph_3Sn(CH_2)_6OH$ (3.85 %) in SBA-15pSn with this M_{50} is approximately 60 times lower than the IC_{50} dosage of free $Ph_3Sn(CH_2)_6OH$. At this concentration, free $Ph_3Sn(CH_2)_6OH$ does not affect tumor cell viability. Impor-

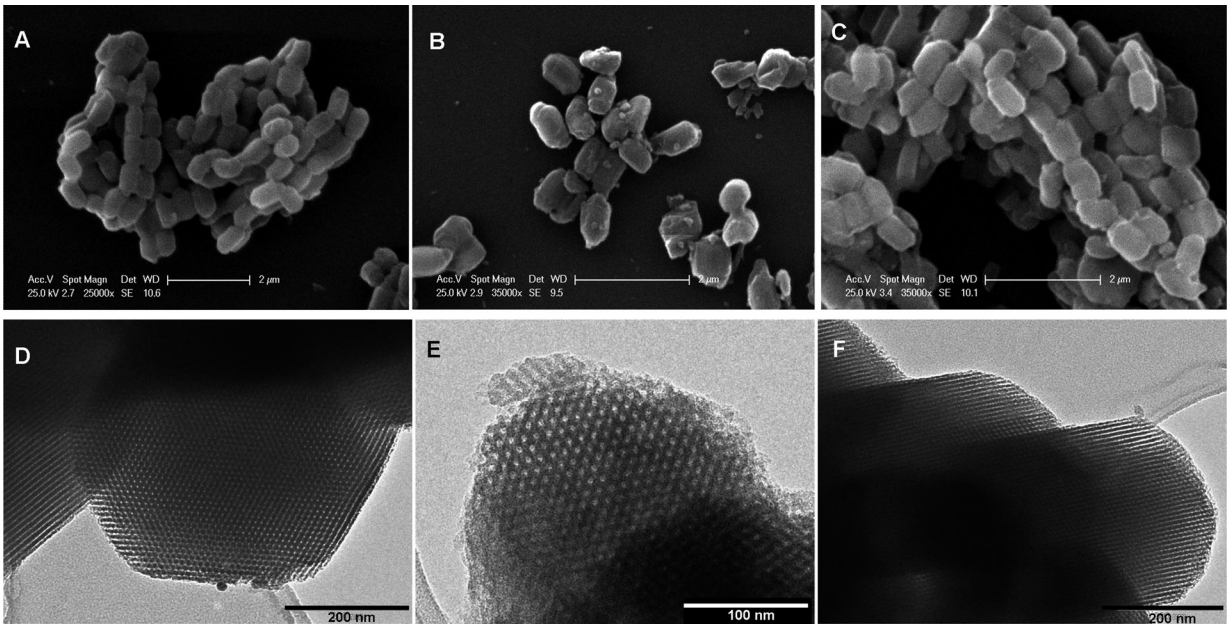

Figure 1. SEM images: A) SBA-15, B) SBA-15p, C) SBA-15pSn; TEM images: D) SBA-15, E) SBA-15p, F) SBA-15pSn.

tantly, carrier SBA-15p alone had no influence on cell viability (Figure S7A and B). Moreover, in contrast to tests with free $Ph_3Sn(CH_2)_6OH$, SBA-15pSn does not affect mitochondrial respiration (according to MTT and CV tests), and thus, the observed decrease of cell respiration is a clear reflection of the decreased number of viable cells (Figure S7A and B).

To investigate the effectiveness of the tested drugs in vivo, B16 cells were inoculated in syngeneic C57BL/6 mice and intraperitoneal treatment started (10th day) when tumors were palpable. At the 28th day, animals were sacrificed. In the control group, four of five animals developed the maximum allowed tumor volume. The tumor growth determined in SBA-15p-treated animals was similar to that of the control. At the same time, two animals of the cisplatin group died during the experiment while two developed tumors of the maximum allowed volume (Figure 2). Whereas in the presence of

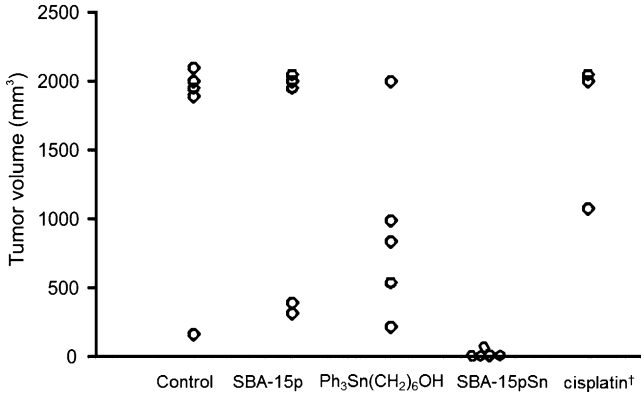

Figure 2. Efficiency of $Ph_3Sn(CH_2)_6OH$, SBA-15p, SBA-15pSn, and cisplatin against mouse melanoma in vivo. B16 cells (1×10^5) were inoculated into C57BL/6 mice ($n=5$ per group); tumor volume after 28 days is shown. † two animals died.

$Ph_3Sn(CH_2)_6OH$ alone, the tumor grows more slowly, indeed, application of SBA-15pSn almost completely abolished the tumor. Biochemical analysis of urine revealed that only cisplatin-treated animals showed serious signs of nephrotoxicity indicated by the presence of erythrocytes and leukocytes in urine as well as elevated level of protein. Based on the apparent absence of toxicity and nephrotoxicity in the SBA-15pSn group in comparison to the cisplatin group, it can be concluded that the tin-loaded mesoporous silica is very well tolerated.

To elucidate the mechanism of antimelanoma action, cells were treated with IC_{50}/M_{50} doses of $Ph_3Sn(CH_2)_6OH$ and SBA-15pSn (obtained from in vitro screening for 72 h), and cell cycle distribution, proliferation, and different types of cell death were evaluated by flow cytometry. Ann/PI double staining revealed the remarkable presence of early apoptotic cells (Ann^+PI^-), while subsequent DNA fragmentation was further confirmed by the accumulation of cells in the subG phase of the cell cycle (Figure S8A and B). The apoptotic process, accompanied by caspase activation in the $Ph_3Sn(CH_2)_6OH$- and SBA-15pSn-treated cultures, was dominant in cells exposed to free $Ph_3Sn(CH_2)_6OH$ alone (Figure S8C).

Interestingly, exposure to SBA-15pSn led to a strong autophagic process manifested through the higher number of autophagosomes in the cytoplasm (Figure S8D). Neutralization of this process by the specific inhibitor 3-MA clearly indicated that autophagy did not contribute to the decrease in cell viability (Figure S8E). Moreover, evaluation of the proliferative potential of surviving cells in cultures exposed to SBA-15pSn by CFSE revealed a strong blockage in first and second division, pointing out the remarkable presence of

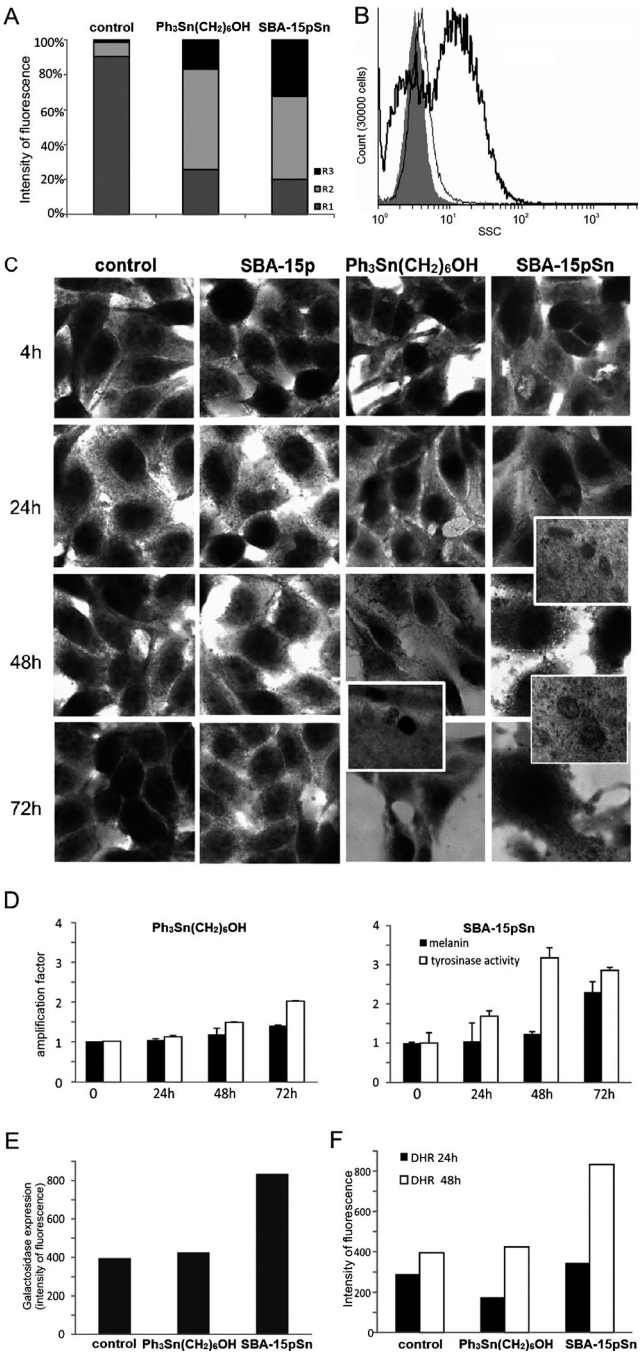

Figure 3. Differentiation of melanoma cells: Cell proliferation (A; R1: first division, R2: second division, R3: undivided cells), granularity of cytoplasm (B), Mayer's hematoxylin-stained cells (C), melanin synthesis and tyrosinase activity (D), galactosidase expression (E), ROS/RNS production (F).

undivided cells (Figure 3A). In concordance with this, an enhanced granularity of cells exposed to SBA-15pSn was observed (Figure 3B). Compared to untreated cells with a round morphology, cells incubated with $Ph_3Sn(CH_2)_6OH$ or SBA-15pSn displayed a flat morphology with an increased volume of cytoplasm and membrane growth resembling dendrites (Figure S9). Microscopic analysis of hematoxilin-stained melanoma cells exposed to tested compounds for 4, 24, 48, and 72 h showed significant differences between cultures treated with SBA-15pSn and free $Ph_3Sn(CH_2)_6OH$ (Figure 3C). While application of $Ph_3Sn(CH_2)_6OH$ mainly promoted apoptosis with all the typical morphological signs, melanoma cells treated with SBA-15pSn underwent differentiation toward melanocytes, marked by the presence of primary and secondary melanosomes,[6a] as confirmed by electron microscopy (Figure S10). This was further supported by measurement of tyrosinase activity as well as melanin content (Figure 3D).

SBA-15p and SBA-15pSn particles were clearly seen within the cytosol of B16 cells even after 4 h of incubation. This is in agreement with previous studies on the mesoporous SBA-15 and MCM-41 particles efficiently ingested by cells.[17] Importantly, their presence in the cell did not promote any visible organelle damage (Figure S10).

Furthermore, loss of malignant properties coincided with enhanced galactosidase expression (Figure 3E), indicating that cells are in the state of senescence. Observed normogenesis could be triggered by reactive oxygen and nitrogen species (ROS/RNS).[18] With this in mind, we analyzed the intracellular level of ROS/RNS and the intensive production of free radicals was detected in cultures exposed to SBA-15pSn (Figure 3F). This phenomenon could be in direct relation with melanoma cell maturation observed upon treatment with SBA-15pSn.

The influence of $Ph_3Sn(CH_2)_6OH$ and SBA-15pSn on the major signaling pathways of B16 melanoma cells was evaluated. Western blot analysis revealed the well-synchronized regulation of Akt and downstream p70S6 kinase in $Ph_3Sn(CH_2)_6OH$ and SBA-15pSn exposed cells. After the initial enhancement in Akt phosphorylation at Ser473 as well as phosphorylation at Thr389 in p70S6k, a site crucial for enzyme activation, this signaling pathway becomes silenced. Its shutting down is also confirmed by the progressive inhibition of autoinhibitory domain phosphorylation at position Thr421/Ser424 which is necessary for maintaining the active p70S6K conformation. This finding is in correlation with the previously found decrease of proliferative potential in cultures treated with SBA-15pSn. Furthermore, ERK1/2

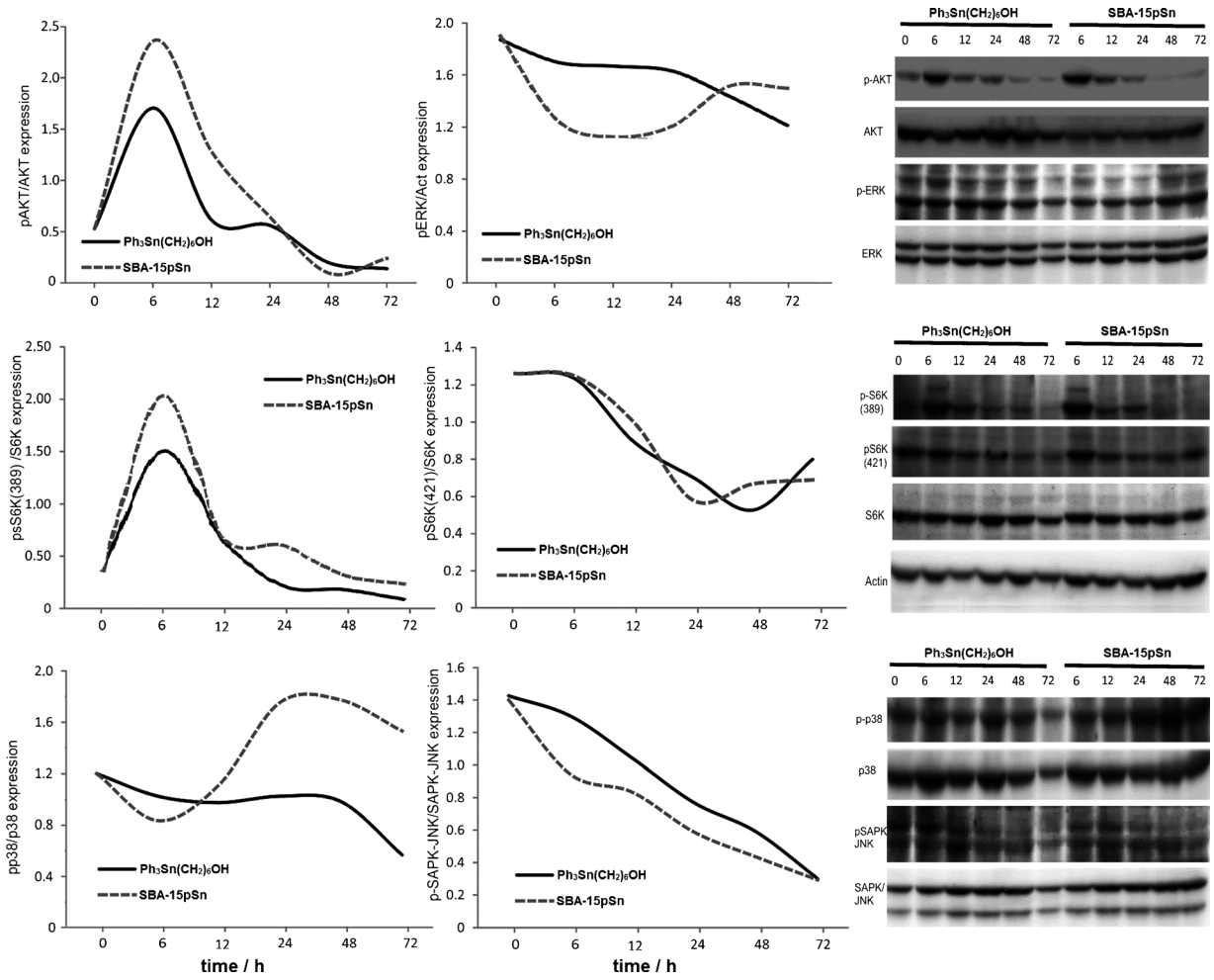

Figure 4. Differentiation of melanoma cells: Intracellular signaling pathways. Western blot analysis of the expressed signaling molecules.

phosphorylation was permanently diminished in response to $Ph_3Sn(CH_2)_6OH$ treatment, while SBA-15pSn (IC_{50} calculated from M_{50} of SBA-15pSn/IC_{50} of $Ph_3Sn(CH_2)_6OH = 1/60$) triggered more potent but transitory ERK1/2 inhibition (Figure 4). A similar pattern of Akt and ERK activity was previously described in B16 melanoma cells in response to the NO-modified HIV protease inhibitor saquinavir, which induces permanent trans-differentiation of these cells into Schwann-like phenotype.[6b] The differentiation of melanoma toward the glial phenotype accompanied with myelin gene expression was previously reported.[19]

Interestingly, in the MAP kinase family, only p38 was affected by free $Ph_3Sn(CH_2)_6OH$ and SBA-15pSn in different ways. While $Ph_3Sn(CH_2)_6OH$ alone continuously inhibited p38 phosphorylation, SBA-15pSn strongly activated this protein (Figure 4). A similar pattern was previously reported as responsible for B16 differentiation.[20] Finally, the last representative member of the MAP kinase family, SAPK/JNK was inhibited by $Ph_3Sn(CH_2)_6OH$ and even more strongly by SBA-15pSn. The down-regulation of JNK activity is very important for the evasion of the compensatory proliferation of cells in apoptotic cell environment. Namely, the induction of apoptosis in the oncotherapy of anaplastic tumors is a "double-edged sword" because dying cells promote the proliferation of their neighbors.[21] This phenomenon was explained by the JNK-dependent production of mitogen mediators which involve JAK/STAT as well as Wnt and Notch signaling.[7] Furthermore, it was documented that JNK inhibition by SP600125 blocked the L-threonine-induced expression of the stem cell marker OCT4 and several cell proliferative molecules, such as cyclin D1, cyclin E, and c-Myc.[22]

In conclusion, we have reported the strong therapeutic potential of organotin(IV)-loaded nanostructured silica (SBA-15pSn) which almost completely abolish B16 tumor growth in syngeneic C57BL/6 mice. More than the drug or the carrier material alone, SBA-15pSn demonstrated dramatically amplified—much more than an additive effect—antitumor activity. Under these conditions, nontoxic doses of the tested drug became highly efficient against melanoma cells. In contrast to the general approach in oncotherapy (induction of apoptosis), SBA-15pSn triggers JNK-independent apoptosis followed by the development of a nonproliferative melanocyte-like phenotype of surviving cells. This pattern of action leads to the nonaggressive suppression of tumor growth with yet nonrecognizable toxicity toward normal tissue.

Received: January 24, 2014
Published online: May 14, 2014

Keywords: cell differentiation · cisplatin · drug delivery · melanoma · nanostructures

[1] L. Kelland, *Nat. Rev. Cancer* **2007**, *7*, 573 – 584.
[2] a) L. Galluzzi, L. Senovilla1, I. Vitale, J. Michels, I. Martins, O. Kepp, M. Castedo, G. Kroemer, *Oncogene* **2012**, *31*, 1869 – 1883; b) E. L. Mamenta, E. E. Poma, W. K. Kaufmann, D. A. Delmastro, H. L. Grady, S. G. Chaney, *Cancer Res.* **1994**, *54*, 3500 – 3505; c) B. Köberle, J. R. W. Masters, J. A. Hartley, R. D. Wood, *Curr. Biol.* **1999**, *9*, 273 – 276; d) J. Y. Djeu, S. Wei, *Adv. Cancer Res.* **2009**, *105*, 77 – 92.
[3] J. Poland, D. Schadendorf, H. Lage, M. Schnölzer, J. E. Celis, P. Sinha, *Clin. Chem. Lab. Med.* **2002**, *40*, 221 – 234.
[4] K. Güven, H. Kittler, K. Wolff, H. Pehamberger, *Melanoma Res.* **2001**, *11*, 411 – 415.
[5] a) D. Wang, S. J. Lippard, *Nat. Rev. Drug Discovery* **2005**, *4*, 307 – 320; b) C.-H. Zhou, Y.-Y. Zhang, C.-Y. Yan, K. Wan, L.-L. Gan, Y. Shi, *Anti-Cancer Agents Med. Chem.* **2010**, *10*, 371 – 395; c) J. Zhang, F. Zhang, H. Li, C. Liu, J. Xia, L. Ma, W. Chu, Z. Zhang, C. Chen, S. Li, S. Wang, *Curr. Med. Chem.* **2012**, *19*, 2957 – 2975.
[6] a) J. Radovic, D. Maksimovic-Ivanic, G. Timotijevic, S. Popadic, Z. Ramic, V. Trajkovic, D. Miljkovic, S. Stosic-Grujicic, S. Mijatovic, *Food Chem. Toxicol.* **2012**, *50*, 3181 – 3189; b) D. Maksimovic-Ivanic, S. Mijatovic, D. Miljkovic, L. Harhaji-Trajkovic, G. Timotijevic, M. Mojic, D. Dabideen, K. F. Cheng, J. A. McCubrey, K. Mangano, Y. Al-Abed, M. Libra, G. Garotta, S. Stosic-Grujicic, F. Nicoletti, *Mol. Cancer Ther.* **2009**, *8*, 1169 – 1178; c) S. Mijatovic, D. Maksimovic-Ivanic, J. Radovic, D. Miljkovic, Lj. Harhaji, O. Vuckovic, S. Stosic-Grujicic, M. Mostarica-Stojkovic, V. Trajkovic, *Cell. Mol. Life Sci.* **2005**, *62*, 589 – 598.
[7] F. Chen, *Cancer Res.* **2012**, *72*, 379 – 386.
[8] a) S. K. Murthy, *Int. J. Nanomed.* **2007**, *2*, 129 – 141; b) D. Peer, J. M. Karp, S. Hong, O. C. Farokhzad, R. Margalit, R. Langer, *Nat. Nanotechnol.* **2007**, *2*, 751 – 760; c) J. D. Rocca, R. C. Huxford, E. Comstock-Duggan, W. Lin, *Angew. Chem.* **2011**, *123*, 10514 – 10518; *Angew. Chem. Int. Ed.* **2011**, *50*, 10330 – 10334; d) C. Wang, Z. Li, D. Cao, Y.-L. Zhao, J. W. Gaines, O. A. Bozdemir, M. W. Ambrogio, M. Frasconi, Y. Y. Botros, J. I. Zink, J. F. Stoddart, *Angew. Chem.* **2012**, *124*, 5556 – 5561; *Angew. Chem. Int. Ed.* **2012**, *51*, 5460 – 5465.
[9] a) H. Summers, *Nat. Nanotechnol.* **2012**, *7*, 9 – 10; b) L. Ma, M. Kohli, A. Smith, *ACS Nano* **2013**, *7*, 9518 – 9525; c) Y. Yan, M. Björnmalm, F. Caruso, *ACS Nano* **2013**, *7*, 9512 – 9517.
[10] a) R. Liu, Y. Zhang, X. Zhao, A. Agarwal, L. J. Mueller, P. Feng, *J. Am. Chem. Soc.* **2010**, *132*, 1500 – 1501; b) C. Y. Lai, B. G. Trewyn, D. M. Jeftinija, K. Jeftinija, S. Xu, S. Jeftinija, V. S. Lin, *J. Am. Chem. Soc.* **2003**, *125*, 4451 – 4459; c) N. K. Mal, M. Fujiwara, Y. Tanaka, *Nature* **2003**, *421*, 350 – 353.
[11] a) L. Li, F. Tang, H. Liu, T. Liu, N. Hao, D. Chen, X. Teng, J. He, *ACS Nano* **2010**, *4*, 6874 – 6882; b) L. A. DeLouise, *J. Invest. Dermatol.* **2012**, *132*, 964 – 975; c) X. Xue, M. D. Hall, Q. Zhang, P. C. Wang, M. M. Gottesman, X.-J. Liang, *ACS Nano* **2013**, *7*, 10452 – 10464.
[12] a) H. Meng, M. Xue, T. Xia, Y.-L. Zhao, F. Tamanoi, J. F. Stoddart, J. I. Zink, A. E. Nel, *J. Am. Chem. Soc.* **2010**, *132*, 12690 – 12697; b) J. M. Rosenholm, A. Meinander, E. Peuhu, R. Niemi, J. E. Eriksson, C. Sahlgren, M. Linden, *ACS Nano* **2009**, *3*, 197 – 206; c) M. Liong, J. Lu, M. Kovochich, T. Xia, S. G. Ruehm, A. E. Nel, F. Tamanoi, J. I. Zink, *ACS Nano* **2008**, *2*, 889 – 896.
[13] a) G. N. Kaluđerović, D. Pérez-Quintanilla, I. Sierra, S. Prashar, I. Hierro, Ž. Žižak, Z. D. Juranić, M. Fajardo, S. Gómez-Ruiz, *J. Mater. Chem.* **2010**, *20*, 806 – 814; b) G. N. Kaluđerović, D. Pérez-Quintanilla, Ž. Žižak, Z. D. Juranić, S. Gómez-Ruiz, *Dalton Trans.* **2010**, *39*, 2597 – 2608; c) S. Sanchez-Munoz, S. Gómez-Ruiz, D. Perez-Quintanilla, S. Morante-Zarcero, I. Sierra, S. Prashar, R. Paschke, G. N. Kaluđerović, *ChemMedChem* **2012**, *7*, 670 – 679.
[14] D. Pérez-Quintanilla, S. Gómez-Ruiz, Ž. Žižak, I. Sierra, S. Prashar, I. Hierro, M. Fajardo, Z. D. Juranić, G. N. Kaluđerović, *Chem. Eur. J.* **2009**, *15*, 5588 – 5597.
[15] For example see: a) G. N. Kaluđerović, H. Kommera, E. Hey-Hawkins, R. Paschke, S. Gómez-Ruiz, *Metallomics* **2010**, *2*, 419 – 428; b) S. Gómez-Ruiz, G. N. Kaluđerović, S. Prashar, E. Hey-

Hawkins, A. Erić, Ž. Žižak, Z. D. Juranić, *J. Inorg. Biochem.* **2008**, *102*, 2087 – 2096.
[16] C. Copéret, M. Chabanas, R. P. Saint-Arroman, J.-M. Basset, *Angew. Chem.* **2003**, *115*, 164 – 191; *Angew. Chem. Int. Ed.* **2003**, *42*, 156 – 181.
[17] Z. Tao, B. Toms, J. Goodisman, T. Asefa, *ACS Nano* **2010**, *4*, 789 – 794.
[18] a) D. Trachootham, J. Alexandre, P. Huang, *Nat. Rev. Drug Discovery* **2009**, *8*, 579 – 591; b) A. R. Ji, S. Y. Ku, M. S. Cho, Y. Y. Kim, Y. J. Kim, S. K. Oh, S. H. Kim, S. Y. Moon, Y. M. Choi, *Exp. Mol. Med.* **2010**, *42*, 175 – 186; c) L. A. Sena, N. S. Chandel, *Mol. Cell* **2012**, *48*, 158 – 167; d) Y. Dong, H. Wang, J. Cao, J. Ren, R. Fan, X. He, G. W. Smith, C. Dong, *Mol. Cell. Biochem.* **2011**, *352*, 255 – 260.
[19] S. G. Slutsky, A. K. Kamaraju, A. M. Levy, J. Chebath, M. Revel, *J. Biol. Chem.* **2003**, *278*, 8960 – 8968.
[20] K. Hata, T. Mukaiyama, N. Tsujimura, Y. Sato, Y. Kosaka, K. Sakamoto, K. Hori, *Cytotechnology* **2006**, *52*, 151 – 158.
[21] C. D. Gregory, J. D. Pound, *Apoptosis* **2010**, *15*, 1029 – 1049.
[22] J. M. Ryu, H. J. Han, *J. Biol. Chem.* **2011**, *286*, 23667 – 23678.

